Low-dimensional structures in silicon and diamond implanted with high-energy ions

Hussein Ali Noor
AL-Qadissiya University/ College of Education
Hussein.ali@qu.edu.iq

Abstract:

Using the method of electronic paramagnetic resonance, the monocrystalline samples of silicon and of natural diamond implanted with high-energy ion was studied. The local magnetic ordering of a system of unpaired electrons has been discovered.

Keywords: (HEI)High Energy Ion; (MR)Magnetic resonance; (EPR) Electron Paramagnetic Resonance.

انخفاض هياكل الأبعاد في السليكون والماس المزروع بالأيونات الطاقة العالية

حسين علي نور
جامعة القادسية

الخلاصة:

تم فحص عينات أحادية من السيليكون والماس بواسطة طريقة الرنين المغناطيسي باراماجنيتيك الطبيعي مزروعة بأيونات الطاقة العالية ف تم اكتشاف وجود ترتيب مغناطيسي موضعي غير نظام الإلكترونات المزدوجة.

الكلمات المفتاحية: ايون الطاقة العالية , الرنين المغناطيسي , الرنين المغناطيسي الالكتروني.

1. Introduction

High-Energy Ion implantation (HEI) is presently a very promising approach to create the deepened doped layers in a semiconductor structures and to realize the increased element density in microelectronic devices due to the formation of multilayer three-dimensional structures. The defect system generated in semiconductor crystals on HEI is differing considerably from the structure formed with low-energy ions. Owing to the increased area and degree of the local material damage characteristic for high-energy (above 1 MeV/nucleon) ion implantation, it is expected that with this implantation new manifestations of different mechanisms associated with the spatiotemporal electron localization and delocalization in the especially high-field case of the long-range ionic action mechanisms, and of the magnetic ordering effects may be revealed[1,3].

2. Experimental method

This work presents a study of silicon and natural diamond samples implanted with high-energy Kr+ and Xe+ ions by the electron Magnetic Resonance (MR)

method. Using of an Electron Paramagnetic Resonance (EPR) spectrometer with a reflective cavity together with the high-frequency magnetic field modulation to establish the magnetic properties have enabled optimization of the recording response and resolution as well as finding the magnetic ordering in relatively thin layers [3].

The objects under study were samples of the p-type Czochralski-grown silicon 0.9-mm thick with the resistivity of 10 Ω· cm (oxygen content ~ 10^{18} cm^{-3}).

Both for silicon and natural diamond, implantation of Xe^+ ions with the energy of 5.68 GeV (dose 5×10^{13} cm^{-2}) and Kr^+ ions with the energy of 210 MeV (dose 3×10^{14} cm^{-2}) was realized at <111> orientation and at room temperature.

To obtain the magnetic centre distribution profile, the layer-by-layer removal in the irradiated area was carried out with the use of a nonmagnetic diamond paste having the grain size below 1 μm.

Thermal stability of the defect structure was determined by means of a 20-minute isochronal annealing at temperature ranging from 370 to 1270 ^oK.

Measurements of magnetic resonance was performed at room temperature using an EPR 3-cm range RadioPAN SE/X–2543 spectrometer at the magnetic field modulation 100 kHz.

3. Experimental results:

The electron MR spectra that recorded for the irradiated samples of silicon represented a superposition of EPR lines for some well-known paramagnetic point defects and also included wide MR lines with the g–factors ranging 2.15 to 2.4, and with the widths ΔBpp ≈ 30 mT for Kr^+ ions and ΔBpp ≈ 20 mT for Xe^+ ions. Besides, the lines with a g–factor of about 3.4 (ΔBpp ≈ 0.3 T) have been observed. No resonance signals were recorded for the initial samples at the same conditions.

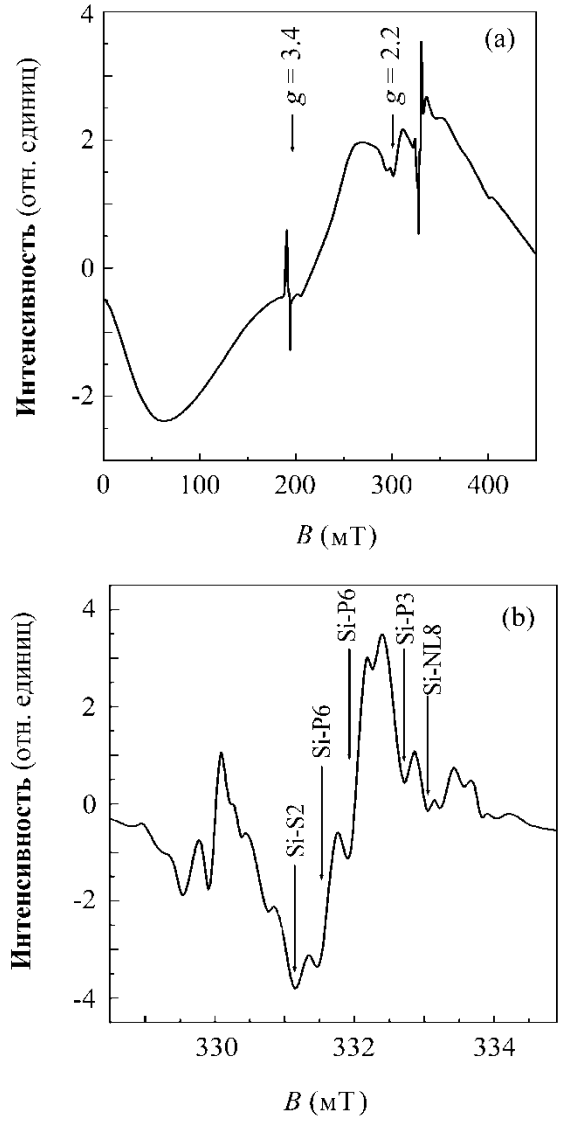

Figure 1. MR spectrum for a silicon sample implanted with Xe+ ions (a).EPR spectrum of point defects (b). The magnetic field is [111]-oriented.

Fig. 1a demonstrates a MR spectrum recorded for the sample implanted with Xe^+ions. The line at B ≈ 0.2 T represents a signal of the calibration ruby (Al_2O_3: Cr^{3+}) sample located at the end wall of the cavity H_{102}. A signal at B ≈ 0.33 T (g = 1.99 – 2.02) is caused by the point defects the structure of which is shown in Fig. 1b.

Analysis of the angular dependences of the g-factor and of the EPR line saturation character has enabled identification of the paramagnetic centres Si-P6 (<100> split *d*-interstice in a positive charge state [1]), Si-S2 (tetra-vacancy in a negative charge state [2]), Si-P3 (neutral (110)-planar tetra-vacancy [3]), thermodonor centres Si-NL8 [4]. The centre Si-P6 is dominant. Each of the indicated radiation centres has a multicomponent spectrum. Some of the lines for such overlapping spectra are arrowed in Fig. 1b.

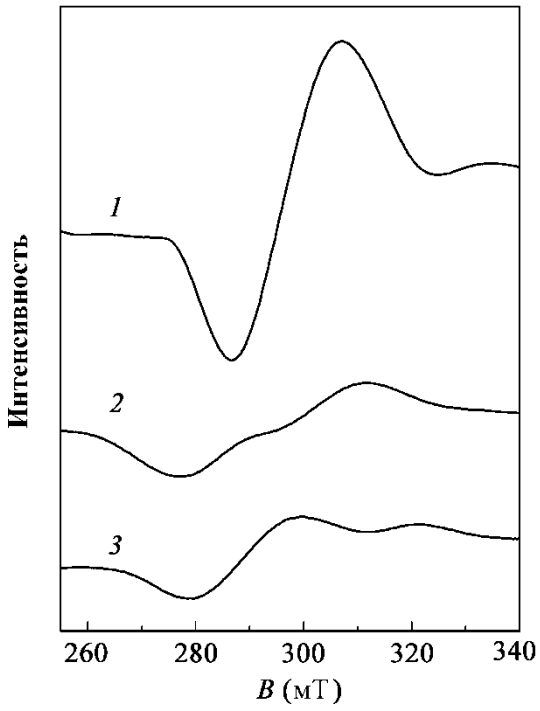

Figure 2. MR signals of a silicon sample irradiated by Xe ions in three successive measurements.

Fig. 2 illustrates the characteristics intensity and MR-signal shape transformation with a g-factor of about 2.2 for silicon irradiated with Xe ions in the case of three successive measurements with a magnetic field scanning time of 8 minutes and with 8-minutes intervals. For the second (signal 2) and for the third (signal 3) measurements in similar conditions, the spectra have revealed a superposition of two lines with the resonance magnetic-field values differing by 20 mT. The appearance of two lines may be due to the local internal magnetic fields differing at the spatially separated sites of the sample. The revealed changing of magnetic resonance lines points to the magnetic accommodation observed in magnetically ordered materials and responsible for the relationship between signals and previous magnetic interactions.

Also, the authors have noticed the difference in values of a resonance magnetic field for wide-band lines when MR is recorded with the increasing or decreasing magnetic-field change. A value of such «hysteresis» dependend on the sample orientation in a magnetic field of 20 – 40 mT for the centres with g ≈ 2.2 and was in excess of 100 mT for the centres with g ≈ 3.4. Similar effects have been observed for silicon samples implanted with Kr ions.

Practically, after removal of the surface layer 4 μm thick in a sample implanted with Xe ions, a wide-band MR line was not recorded for g ≈ 3.4.

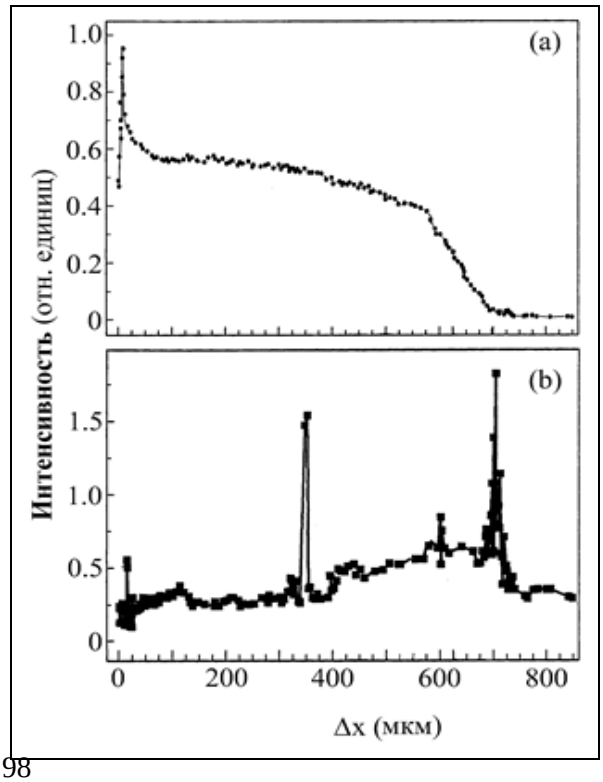

Figure 3. Measuring of the EPR signal intensity for point defects (a) and of the MR signal at g of about 2.2 (b) as a function of the removed layer thickness Δx.

The intensity changes of the MR signal with a g-factor of about 2.2, normalized to the calibration sample signal, resulted from layer-by-layer removal of the irradiated area are given in Fig. 3. Besides, this figure presents similar changes of the total EPR signal intensity for point defects. As seen, a signal of point defects decreases monotonically as the irradiated layer is removed, disappearing practically after removal of the layer 700 μm thick. Point defects are observed to the depth slightly exceeding the average projective range (616 μm).

Other situation was observed for the MR signal with g ≈ 2.2 whose parameters are changing non-monotonically after layer-by-layer removal of the irradiated area. In Fig. 3 b, it can be seen that removal of the layers with a thickness of 15, 350, and 703 μm leads to a drastic increase of the intensity followed by its decrease and to the corresponding changing of the g-factor (up to 10%). As distinct from EPR lines for point defects, the MR signal with g ≈ 2.2 was invariable after removal of a layer 800 μm in thickness.

No significant changes in the parameters of a signal for the magnetic centres with g at about 2.2 were observed after annealing at 1270 ^{0}K. But the retained «hysteresis» points to the fact that a defect system holds its magnetic properties even after such high temperature treatment.

EPR signals of point defects were recorded for the irradiated diamond crystals as well. Besides, the specific signals of electron magnetic resonance for the regions with an elevated degree of radiation disordering have been recorded.

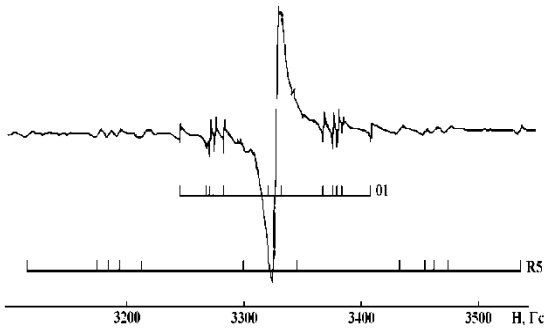

Figure 4. Electron paramagnetic resonance spectrum of natural diamond.

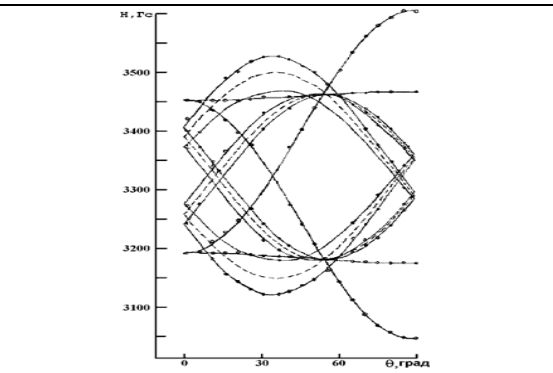

Figure 5. Angular dependence of the spectral line position for PC of a high-field series.

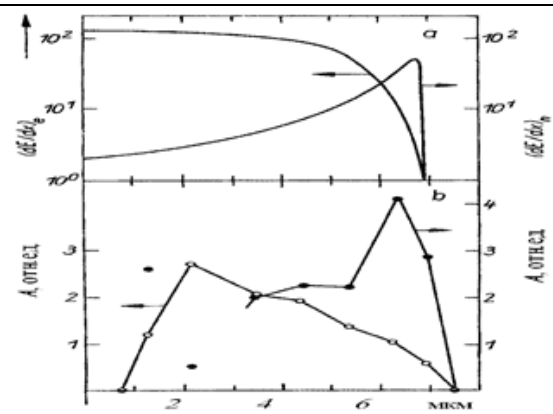

Figure6. The in-depth impurity distribution profiles: computed using TRIM -96 (a) and experimental (b).

line at the centre of the spectra for both non-annealed and annealed (at 600…1100 °C) samples [5] is due to

absorption by the quasi-particles following the tracks of high-energy electrons and similar to the topological solitons [6]. Two series of the lower-intensity and heavily anisotropic lines (Fig.4) belong to the point centres known for irradiated diamond.

4. Results and discussion

It is of interest whether the hetero-junctions between the spatially ordered 3D–phase (crystal matrix) and 1D–phase (tracks) generated due to high-energy implantation are abrupt, involving a limited range of the defect types, or there is a vast region with a number of the intermediate, transitional structural defect forms. In principle, EPR data are valuable for solution of this problem as anisotropic studies of EPR spectra enable one to establish a symmetry of the particular paramagnetic centres (PC) and a point symmetry group of the crystal lattice itself (accurate to within the inversion operation of C_i).

Indeed, in the samples under study both series of resonance anisotropic lines may be described by the spin Hamiltonian $\boldsymbol{H}$ as follows[7]:

$$\boldsymbol{H} = \beta \mathbf{H} \mathbf{g} \mathbf{S} + \mathbf{S} \mathbf{D} \mathbf{S}, \qquad (1)$$

where D and g — fine structure tensor and g–tensor, respectively; S — spin operator, H — external magnetic field, β — Bohr magneton.

Following the from analysis of the angular dependence that shown in Fig. 5, the centres are of C_{2v}-type symmetry at the lattice having a point group symmetry no lower than T_d. Since the groups T_d and $O_h = T_d \otimes C_i$ are indistinguishable in magnetic resonance studies, the above means that, in fact, these centres could be considered as point centres of the diamond lattice.

The centres with a high value of fine splitting are known as D–R5 [5]. The data of [7] are in good agreement with a model treating D–R5 centres as <110> three-vacancy complexes V3. The unit spin of D–R5 centre is due to the dipole-dipole interaction of two unpaired spins positioned at the orbitals of different carbon atoms which, in this centre, are located at a distance of 0.47 nm from each other. An additional argument in favour of the vacancy model for D–R5 centre is the increased value of its specific coefficient of the fine splitting growth with the annealing temperature as compared to that for D–01 centre associated with lines of the second series, see Fig. 4. The average value of this coefficient over the interval 600…1100 °C comes to ~0.02 Gsp/K at the orientation <110>. A similar value is observed for D–O1centre: ~0.01 Gcp/K. High coefficients of the spectroscopic parameters variation with the annealing temperature are characteristic for the vacancy centres and for the optical range [5].

The situation is sliqhtly different for the centre D–O1. As demonstrated by analysis of the relation between the components of g-tensor according to the Lee-Corbette principle [7], these centres should include impurity or interstitial atoms. The centres D–O1 have been observed after implantation of different ions into the samples with various qualitative and quantitative impurity compositions. Because of this, impurity atoms the implanted atoms including should not be part of the centres. In their

case the g–tensor and the fine-structure tensor are related by

$$D_{ij} = ½ \lambda \Delta g_{ij}, \quad (2)$$

where D_{ij} — components of D tensor; i, j = 1, 2, 3; Δg_{ij} — components of the tensor $\Delta g = g–2.0023$ E, E — unit matrix.

Fulfillment of relation (2) may be an indicative for the fact that the unit spin, as distinct from D-R5 centre, is formed by orbitals of a single carbon atom only. A high localization degree of the wave function for the centres indicates that the layer-by-layer removal method may be used to establish a profile of the center concentration distribution in ion track length from the sample surface.

As seen in Fig. 6, the concentration distribution profile of D–O1 centres correlates well with a theoretical profile for distribution of the ion energy released on interaction with the crystal electron subsystem. Consequently, the D–O1 center formation and localization mechanisms may be related to formation mechanisms of the tracks representing, at a major portion of their length, nanotubes in the diamond matrix.

It is known [8-9] that high-energy implantation in a single crystal of silicon results in the formation of a heterogeneous defect structure along the ion tracks and its density is lower than that of the matrix. Several types of the defect structures are formed, as rule spatially separated and thermally stable, surrounded by the single-crystal matrix containing point defects. Substructures with a high degree of disordering comprise the one-dimensional inclusions resultant from electron retardation of high-energy ions, regions of their overlapping, two-dimensional substructures emerging in the region of nuclear deceleration of the ions at the end of their track. Just as a result of a spontaneous re-crystallisation within the limits of the one-dimensional inclusions (ion tracks) a stable system may by formed from disordered crystalline grains with the increased local density of «dangling bonds» at the interfaces. An additional source for the formation of two-dimensional thermally stable structures with the increased structural imperfection is the mechanical effect on the area implanted with high-energy ions in the process of its layer-by-layer removal. This effect is of great importance during the treatment of implanted crystals (see Fig. 3b), being less important for the layer-by-layer removal of non-irradiated crystals. It seems natural that precisely in the heavily disordered substructures there is a concentration of the sites featuring a high local density of unpaired electrons.

To some extent, the one-dimensional silicon structure with the lowered atom density lying along the high-energy ion track is similar to the one-dimensional hollow structure in diamond that is also embedded into the single crystal matrix. This substructure is referred to as the track in analogy with the well-known fullerene-like nanotube [10]. Its specific structural and magnetic resistance properties are analyzed in the survey paper [5]. It has been found that a system of unpaired electrons with the increased local spin concentration in diamond, unlike silicon, reveals a specific form of the collective magnetic ordering that leads to the formation of magnetic-resonance solitons.

5. Conclusion:-

As demonstrated by the experimental results, the defect structure in diamond and in silicon on high-energy ion implantation

has some specific features. First, it is anisotropic. Second, this structure reveals the local magnetic ordering associated with the one-dimensional and two-dimensional «island» inclusions with a high local concentration of unpaired electrons present within the matrix. The defect structures generated due to high-energy implantation feature the formation of spatially separated inclusions having different degrees of magnetic ordering. Both in diamond and in silicon, the ion track structure is stable even where experiencing the annealing temperatures up to 1000 °C.

6. Reference

[1] Lee, Y.H. N.N., Gerasimenko in J.W. Corbett,(EPR study of neutron-irradiated silicon: A positive charge state of the <100> split di-interstitial, Phys). Rev. B 14 (2009) 4506-4520.

[2] Brower K.L., Beezhold W.S.,(Electron paramagnetic resonance of the lattice damage in oxygen-implanted silicon), j. Appl. Phys. 43 (1972) 3499-3506.

[3] Lee, Y.H. J.W. Corbett,(EPR study of defects in neutron-irradiated silicon: New-in alignment under uniaxial stress <100>, Phys). Rev. 9 (1974) 4351-4361.

[4] Gregorkiewicz, h.h., . Ammerlaad P.Th., Bekman C.A.J, (Comparative study of Si and Si-NL10 NL8 thermal-donor-related BLIND centers, Phys). Rev. B, 41 (1990)-12636 12628.

[5] Efimov V. D.p., Stelmach V.f. (ESR-spectroscopy of low-dimensional structures by ion implantation in natural diamonds and synthetic diamond films (review)), JPS, 64, no. 4 (1997) 421-449.

[6] Schrieffer J.R., Heeger A.J.(Soliton excitations in polyacetylene. Phys). Rev. B, v. 22 (1980) 2099.

[7] Gelfand, R.B. Erchak, D.P., Penina N.M., Tolstykh V.P., Ulyashin A.G., Varichenko V.S., Zaitsev A.M.(paramagnetic defects in diamond Point irradiated by high energy ions. Phys).stat. Solidi (a), (V) 121, N1 (1990), 63-72.

[8] Chelyadinski A., Varičenko V.s., Zaitsev a.m.,(spatial distribution, accumulation and annealing of radiation defects in Silicon implanted by high-energy ions, krypton and xenon), FTT 40 (1998) 1627-1630.

[9] Varičenko, V. Drozdov, N.m. Lapčuk, E.n. Sat. Rep. (III) (International. Conf. "The interaction of radiation with a solid" WITT-1999), Minsk, 1999, part 1, pp. 95-97.

[10] Erchak V.D (fullerenopodobnye structure of Fullerenes in condensed media). Tez. Rep. -Minsk: «Tehnoprint», 2002. -224 s.